GBT Memo 255

Astronomical Results from the Recommissioning of the Ka-band as a Dual-Feed, Single Channel Receiver using the Spectrometer

Ronald J Maddalena, D.J. Pisano, Jeff Wagg
December 20, 2007

Background

Following the Winter 2006-2007 season, it was determined that the Ka-band (26-40 GHz) receiver's performance, while adequate for science observations was not stable enough for detecting broad, weak lines (GBT Memos 245,246[1]). Subsequent lab testing during Summer 2007 suggested that asymmetries in the input circuit due to the geometry of the OMT were the cause of these instabilities (GBT Memo 248, 249). Therefore, the receiver was redesigned to have symmetric signal paths with only one polarization provided per feed. This new configuration provides benefits for deep observations of broad, weak lines with the Zpectrometer and Spectrometer backends. In addition to the receiver changes, subreflector nodding as a standard observing mode was also implemented during Summer 2007.

This memo reports the results from the recommissioning activities and shared-risk science observations during Fall 2007 using the Spectrometer and subreflector nodding. Results from the CCB and Zpectrometer commissioning observations will be reported elsewhere.

GBT Memo 246 reported that the two hybrid states of the receiver must be calibrated separately to properly account for gain differences between the signal paths. Furthermore, vector T_{cal} calibration was shown to produce far better baseline stability than scalar calibration. Because these results are independent of the receiver configuration, these issues are not revisited in this memo.

Software, Routing, Setup, GFM

The recommissioning activities included testing the software for any problems due to changes in the receiver configuration and the new software developed for subreflector nodding. Unlike Spring 2007, when we had to nod the subreflector using a combination of inputs from Astrid and CLEO, for these observations subreflector nodding is now an integral part of Astrid. We also had to determine how the two removed channels affected cabling, IF Manager, GFM, config-tool, and the number of spectral windows one could observe simultaneously

After making some changes to config-tool, and correcting an oversight in the cabling file, all problems were resolved. Routing and labeling by the IF Manager are correct. A positive, unforeseen consequence of the changes to config tool is that one can use four 200 or 800 MHz

[1] GBT memos are available online at http://wiki.gb.nrao.edu/bin/view/Knowledge/GBTMemos

spectral windows simultaneously. A minor negative is that GFM complains that it cannot process pointing data in the default manner (using only the L polarization from both feeds). Nevertheless its fallback algorithm does process the data correctly (using the only signals being passed to the DCR).

All Ka-band observers need to be aware of the following config-tool changes. These changes require that the observer specifies beam='B1' in their config files. Last year, with the two channel receiver, one specified 'B12'. Specifying B12 may not provide a routing to the DCR that GFM can process. It also will reduce the number of possible spectral windows from four to two. This change does not affect the selection of the beam to be used for pointing the telescope, for example as an input to a Track or Nod command.

Subreflector Nodding

As reported in GBT Memo 246, subreflector nodding on a rapid timescale (9 second cycle times) can produce better baselines than traditional nodding. To test this in Winter 2007, we had to jury rig a system that depended on Astrid to configure the subreflector segments, while scans had to be run from the Scan Coordinator in CLEO. This method was used because Astrid would clear all segments of the subreflector before each scan started (halting the nodding). This "feature" of Astrid was removed over the summer while a more elegant solution was implemented. The initial tests of the Ka-band receiver used this mode of subreflector nodding. With the M&C release version 7.6, a new *submotion* parameter was added that allows a user to specify the motion of the subreflector. This parameter was wrapped within a new Astrid command, *SubBeamNod*, which uses the subreflector to nod between the two beams of any dual beam receiver. Comparing the flux of 3C286 when observed with traditional nodding and both implementations of subreflector nodding yield equal fluxes (within errors).

Subreflector nodding improves spectral baselines for wide-line observations. These improvements are not necessary for narrow-line targets, so subreflector nodding is not necessary for these observations. For the shortest cycle times allowed (about 9 seconds for a full cycle), the overhead (3 seconds) is identical, as a fraction of the observing time, to traditional nodding; for longer cycle times the overhead will still be 3 seconds, so the relative fraction will be lower. *Therefore, while narrow line observers may not reap the benefits of improved baselines from subreflector nodding, they can improve their overhead by using such nodding with longer cycle times.*

Wide-line observers will benefit from short cycle times, but may, under certain weather conditions, wish to use longer cycle times to improve overheads with minimal degradation of baseline shapes. Based on observations taken as part of project GBT05-030, there is an improvement in the rms noise for longer cycle times (as expected due to reduced overhead), but no significant improvement in baseline shapes for faster nodding in good weather conditions. Further study is needed on the effects of different cycle times on the baseline shapes as a function of weather conditions, but for now we can recommend that half-cycle times of order 18 seconds should be sufficient for most observers. The minimum half-cycle time is 4.4 seconds or 3 integrations of the Spectrometer.

Here is a quick summary of how to specify subreflector nodding in Astrid. For Spectrometer and DCR (devices for which Astrid can obtain the actual data dump times), use the syntax:

- SubBeamNod(source='3C286', scanDuration=60, beamName="MR12", nodlength=3, nodunit="integrations')

This is equivalent to:

- Track('3C286',None,60.,"MR12",submotion=SubNod(3,'integrations'))

In both cases we are nodding between beams 1 and 2 on a dual beam receiver, say Ka-band, with 3 integrations per half cycle for a 60 second observation. This time can also be specified in seconds, and must be for devices that do not provide Astrid with their integration time. For such devices (CCB, Zpectrometer, or other user backends), specify the half-cycle time in seconds using:

- SubBeamNod(('3C286',None,60.,"MR12",nodlength=4.9645423,nodunit='seconds')

All Astrid observing commands can take a *submotion* argument, but we suggest that most observers use *SubBeamNod*.

There are limitations to subreflector nodding, however. **OBSERVERS MUST NOT SUBREFLECTOR NOD FOR MORE THAN 45 MIN**. After 45 min, grease actuators using a Focus or Point & Focus observation. **At present, subreflector nodding is only released for Ka-band observations.** In the future it will be available for general use with all dual beam receivers. Also, in the future it may be possible to use the subreflector for more complex motions and for doing position-switching at low frequencies, but there are no current plans to implement either of these modes in the near future.

A number of tests have revealed power offsets of ~30mK between the two positions of a subreflector nod that is not present with traditional nodding. The general belief is that this is due to ground spillover effects, but further investigation of this issue is ongoing.

Commissioning Observations

On-sky tests of the re-configured Ka-band receiver took place in late September and early October of 2007. Data were taken as part of the TKA project on September 25, 28, and 29 and October 10 and 21. We report on the results below.

T_{cal} & T_{sys} Measurements

We have taken SCAL measurements toward 3C286 and 3C48 that went from 26 to 40 GHz; the two observations agree to within 5%. Figures 1 and 2 are the 3C286 T_{cal} plots and Galen Watts's lab measurements. The weather conditions for both were the 30 percentile winter

weather conditions (i.e., the weather is better only 30% of the time). The data are corrected for frequency dependent gains and opacities, which ranged from 0.04 to 0.075 across the band.

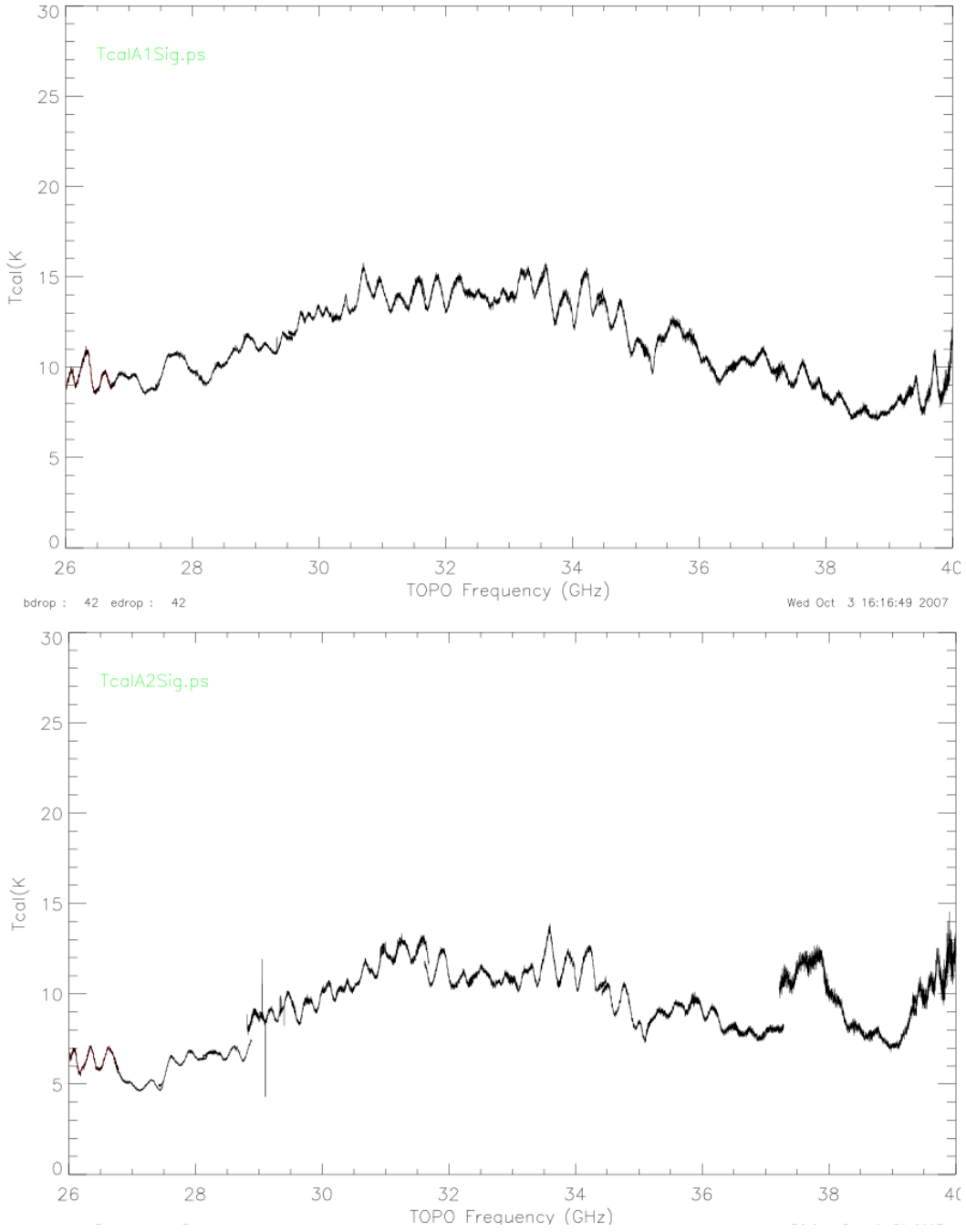

Figure 1: Noise diode values determined astronomically from observations of 3C286. The top panel is for the R1 channel, the bottom for L2. Both are with the hybrid in its 'signal' phase.

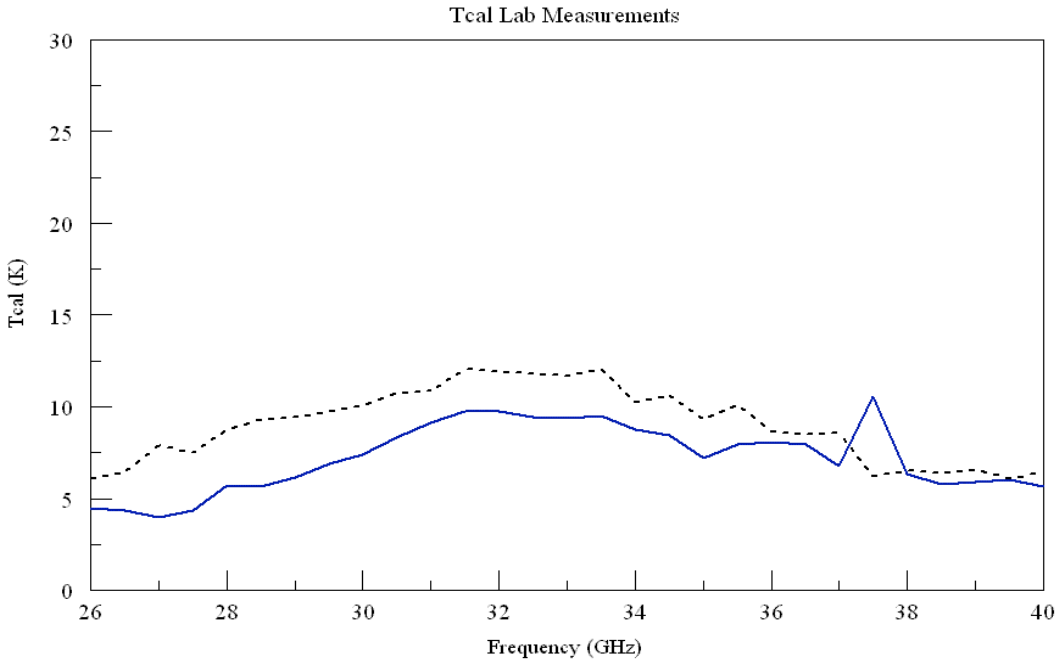

Figure 2: Noise diode values determined from laboratory hot-cold load tests. The dashed curve is the R1 channel, the solid is L2

The frequency structures of Tcal are vastly improved over that of the previous dual channel receiver (see figures 8 -11 in GBT Memo 246) and are not much worse than Q-band's T_{cal} structure. The diode has adequate power across the full 26-40 GHz. T_{cal} is ~ 1/6 of T_{sys}. For most receivers, T_{cal}/T_{sys} = 1/10 is the target level, but we are not suggesting any modifications be made this season. The lab T_{cal} values are about 20% lower than those measured astronomically, which is a bit larger discrepancy than typically.

The frequency structure of T_{sys} (Figure 3) is also vastly improved over that of last spring's receiver (see figures 12-15 in GBT Memo 246). There remains a 300 MHz ripple throughout most of the band which will appear as a ghost in most wideband observations. Ripples are noticeably different for the two channels -- they are worse between 35-37 GHz for R1, and worse between 29-31.5 and 37-38 GHz for L2 . Since 300 MHz ~ 3000 km/s, the frequency structure of the ghost is much wider than the width of most expected lines (< 600 km/s). Thus, the ripple should have minimum impact on wide-line searches.

T_{sys} is 'good' all the way up to ~39 GHz, above which the Q-band receiver has better performance. The minimum is 35 K and increases toward the high end of the band where the atmosphere contributes about 11 K to that increase. For the limited frequency range over which the old design worked, T_{sys} are 10 K lower with the new receiver than with the old, or a 25% improvement. Over much of the band, the new T_{sys} values are much lower than the old. On days with weather better than the ones under which these data were taken, the percentage improvement in T_{sys} will be higher than 25%.

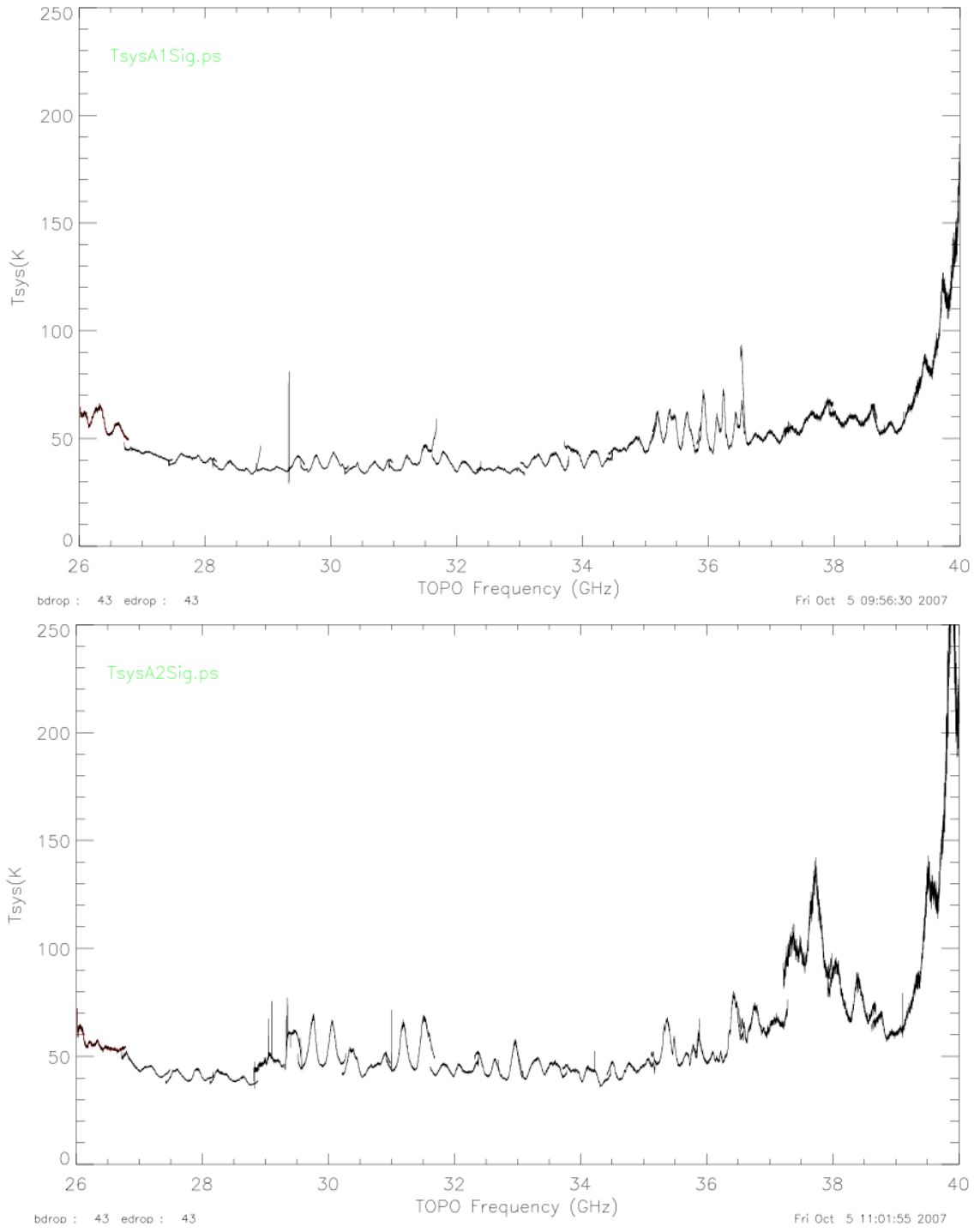

Figure 3: System temperature values as determined from astronomical observations using the noise diode values in Figure 1. The top panel is for the R1 channel, the bottom is for the L2 channel. Both are with the hybrid in its 'signal' phase.

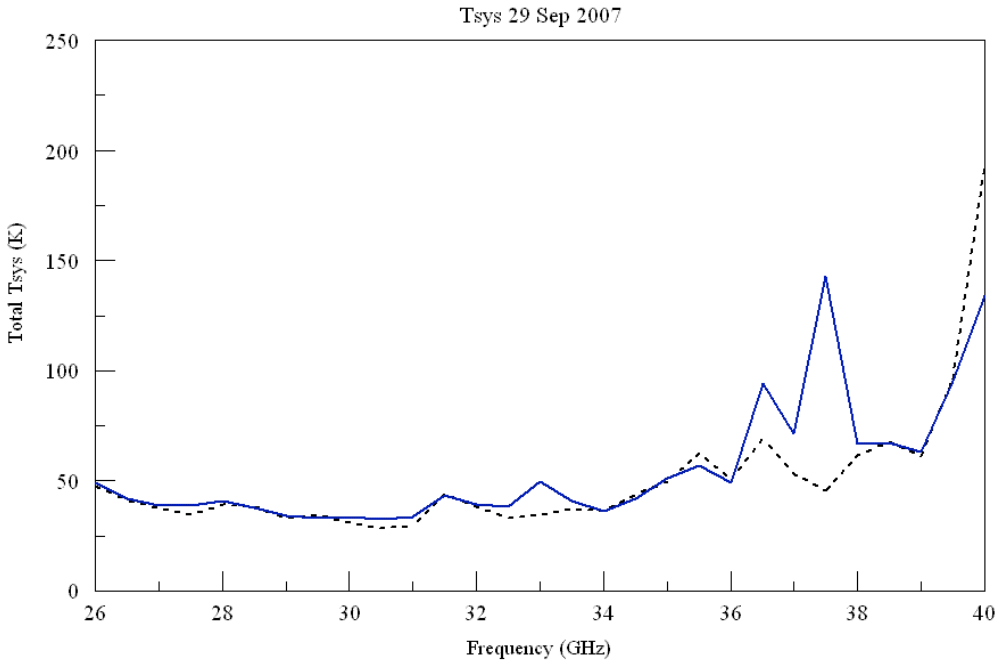

Figure 4: Estimated system temperatures using the values of the receiver temperature derived from lab measurements using hot-cold loads, plus an estimate of the contribution to system temperatures from the weather conditions and elevations of the 3C286 observations, plus 6 K as a best guess for the contributions from the CMB and spillover. The dashed curve is the R1 channel, the solid is L2

Lab T_{Rcvr} measurements, plus a model of the atmospheric contributions to T_{sys}, imply a T_{sys} (Figure 4) that is, to within the uncertainties, the same as what is measured astronomically.

As shown below, any ripples in T_{sys} can end up as ripples in long integrations. Although the ripple will have minimum impact on astronomy, we should at least investigate the cause of the ripples. Galen has already determined from lab measurements that exchanging the mixers that sit right after the hybrid can have a detrimental affect on T_{sys} around 36-38 GHz. Note that these frequencies cover most of the places in the T_{sys} spectrum where the ripples have the highest magnitudes.

If you compare Figure 3 and 5, where the hybrid is in its 'signal' and 'reference' phase, respectively, one easily notices that there is a strong correlation of the ripples in the R1 'signal' phase data with the L2 'reference' phase data. Similarly, the ripples in T_{sys} for the R1 'reference' phase are highly correlated with those from the L2 'signal' phase data. It is not apparent that there are any strong correlated ripples between R1 'signal and R1 'reference.

This is strong evidence that the ripples across the whole band are arising from someplace after the hybrid. As Figure 6 shows, R1 'signal' and L2 'reference' share only the path labeled G_{IFA1}. Similarly, L2 'signal' and R1 'reference' share the path labeled G_{IFA2}. (R1 'signal' and R1 'reference' share G_{R1} only; L2 'signal' and L2 'reference' share G_{L2} only.) The high correlation between R1 'signal' and L2 'reference' but the lack of strong correlation between R1 'signal' and R1 'reference' implies that frequency structures in G_{IFA1} are the major cause of the R1 'signal' and L2 'reference' ripples. Likewise, the high correlation between L2 'signal' and R1 'reference' but the lack of strong correlation between L2 'signal' and L2 'reference'

implies that frequency structures in G_{IFA2} are the major cause of the L2 'signal' and R1 'reference' ripples.

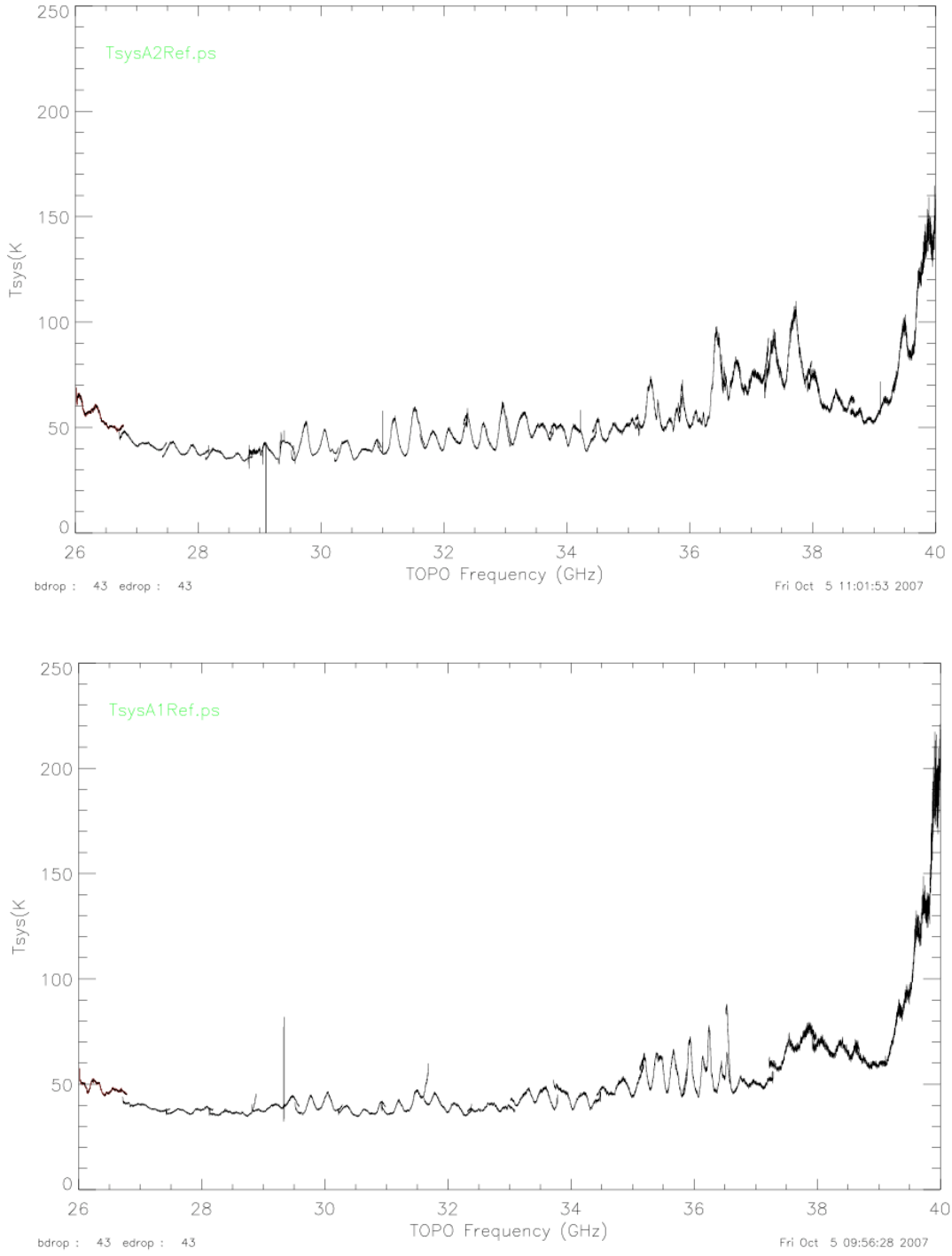

Figure 5: System temperature values as determined from astronomical observations using the noise diode values in Figure 1. The top panel is for the R1 channel, the bottom is for the L2 channel. Both are with the hybrid in its 'reference' phase.

Note that G_U, G_{R1} and G_{L2} may also be producing ripples in T_{sys} but they must be of a much lower magnitude than those arising after the hybrid. The Zpectrometer may not see the ripples presented here because Zpectrometer taps into the signal path in a different way than does the Spectrometer.

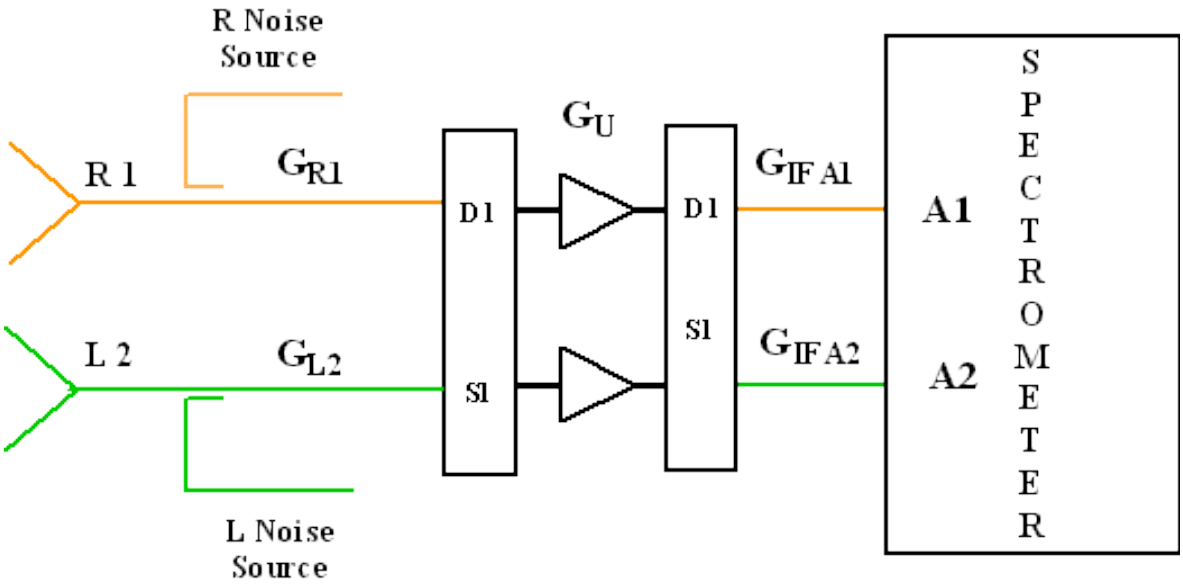

Figure 6: Very simplified schematic of the current receiver design.

Astronomical Observations

We have nearly 16 hrs of observations of high redshifted CO and HCN from two objects at 32 GHz and 34.5 GHz for two projects GBT 05A-029 and GBT-05C-003. The calibrated, but un-baselined data are shown in Figure 7, while the baselined result is shown in Figure 8.

The ripple in Figure 7 appears to be some combination of, mostly, a ghost of the T_{sys} ripple plus another ripple of unknown cause. Our first attempts at using the measured T_{sys} to model out the ripple were only partly successful. Since the expected line width (500 km/s) is much narrower than the ripple period, this structure will not compromise most experiments. Traditional polynomial fitting should be sufficient to remove the residual structure for most observations.

The CO observation in Figure 8 shows a 4 mK, 5-sigma detection in just under 4 hrs of telescope time. The width (500 km/s) and center frequency are exactly as expected. This was daytime observing when the wind was gusting to over 10 mph. We were using the time to test baselines, and not trying to get a detection so the flux scale is arbitrary. Nevertheless, these data demonstrate the improved quality of the baselines.

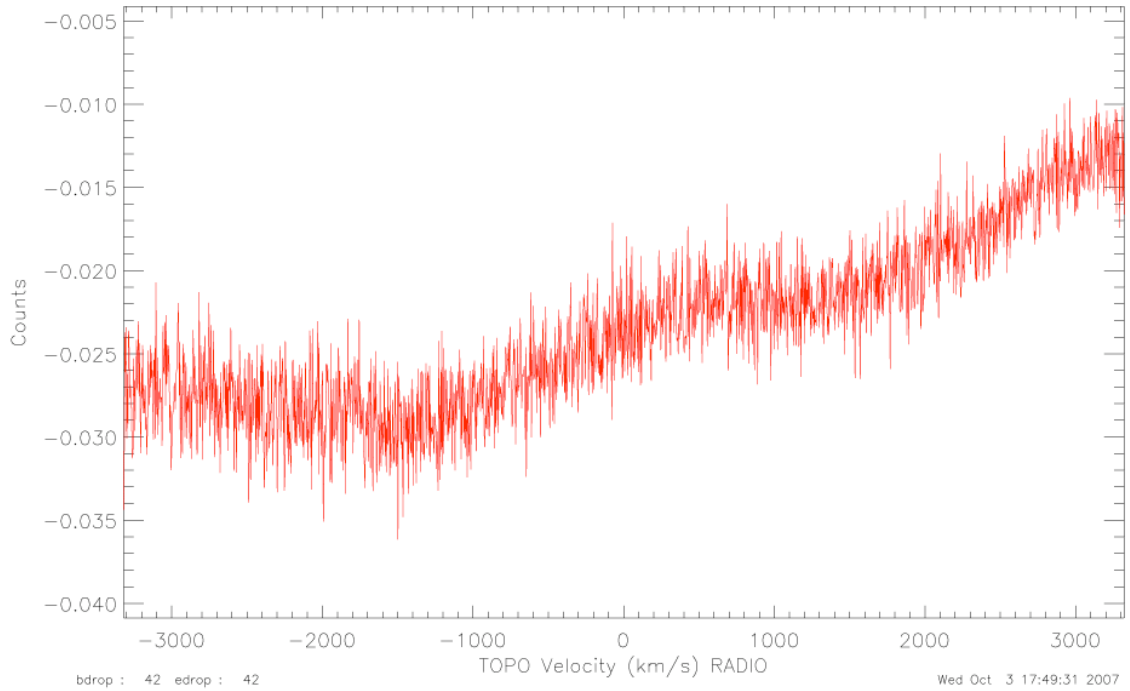

Figure 7: Calibrated but un-baselined data from 7.5 hours of observing at 34.5 GHz in units of T_A.

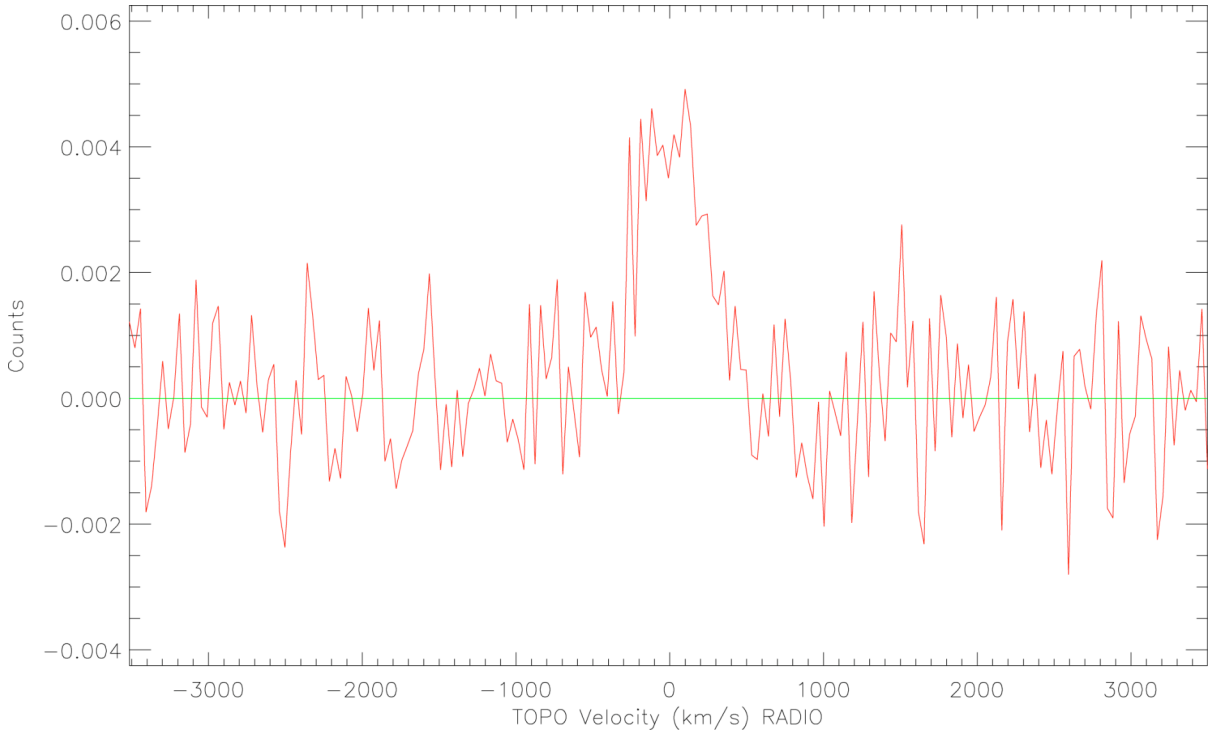

Figure 8: Calibrated, baselined data from 2 hours of observing CO (1-0) from a z=2.56 quasar in good weather conditions in units of T_A.

The rms noise level over a small (50 MHz) frequency range in the spectrum is a about 30% higher than that predicted by the radiometer equation. Our best guess is that the excess noise

arises from the calibration process. Currently, we are weighting all scans equally and not weighting by system temperature when averaging the data. Since some observations were taken over a large range of elevations, a proper weighting would reduce the noise probably by about 10%. We are also using a T_{cal} vector, derived from astronomical data, which is probably insufficiently smoothed.

Summary

The new receiver has far superior frequency coverage. For the limited frequency range over which the old design worked, T_{sys} improvements aren't as great as we initially hoped (~1.4x lower) but are still significant (~1.25). The loss of the second channel is almost but not fully compensated for by the reduced T_{sys}. To achieve the same noise levels as with the dual channel receiver, observing times would need to be increased by 20% to 30% for 10 and 50 percentile winter weather conditions, respectively.

However, this scaling only applies to a subset of observations that would take place in the limited frequency range where the old receiver had good performance. Many narrow line experiments could not be performed with the old receiver because of its limited frequency coverage and T_{sys} ripples. In comparison to the old receiver, the T_{sys} ghosts in baselines should be much lower, thanks to the lower magnitude frequency structure, and less problematic (due to the frequency scale of T_{sys} ripples). The major cause of the ripple must lie after the hybrid.

Thus, there is only a small subset of projects that would find the performance of the new design less favorable than the old.

Future Work

A number of software improvements for the Ka-band receiver and subreflector nodding observations have yet to be implemented. Specifically, we will need to finalize the GBTIDL reduction routines for doing scal measurements, *getscalKa*, and to reduce nodding data, *getnodKa*. We need to adapt the receiver manager, IF manager, config-tool, and GFM in order to accommodate the single channel receiver. The config-tool must also be modified to properly set the LO1B frequency so that it will not produce an interfering signal for observations following Ka-band observing and to place the LO1B frequency into the center of the MM-wave converter's useful frequency range. These improvements will be done as part of ongoing software maintenance as manpower allows.

The current architecture of the W-band (68-86 GHz) receiver is the same as the original Ka-band design. Given our experiences with the Ka receiver, we will need to consider what changes, if any, to make to the W-band design before building it. The results in this memo and previous ones as well as the data taken for the recommissioning should help to inform this decision.